Cell, Vol. 106, 233–241, July 27, 2001, Copyright ©2001 by Cell Press

The Path of Messenger RNA through the Ribosome

Gulnara Zh. Yusupova,[1,4] Marat M. Yusupov,[1,4] J.H.D. Cate,[2] and Harry F. Noller[1,3]
[1] Center for Molecular Biology of RNA
Sinsheimer Laboratories
University of California, Santa Cruz
Santa Cruz, California 95064
[2] Whitehead Institute
Cambridge, Massachusetts 01242

Summary

Using X-ray crystallography, we have directly observed the path of mRNA in the 70S ribosome in Fourier difference maps at 7 Å resolution. About 30 nucleotides of the mRNA are wrapped in a groove that encircles the neck of the 30S subunit. The Shine-Dalgarno helix is bound in a large cleft between the head and the back of the platform. At the interface, only about eight nucleotides (−1 to +7), centered on the junction between the A and P codons, are exposed, and bond almost exclusively to 16S rRNA. The mRNA enters the ribosome around position +13 to +15, the location of downstream pseudoknots that stimulate −1 translational frame shifting.

Introduction

Genetic information is presented to the ribosome in the form of messenger RNA (mRNA), whose codons are read by base pairing with transfer RNA (tRNA) during protein synthesis. Besides its interactions with tRNA, the mRNA also interacts with the small subunit of the ribosome. About thirty nucleotides of mRNA are sequestered by the ribosome (Steitz, 1969), through interactions that influence proper reading of the encoded message. In prokaryotes, selection of the correct start site is guided by base-pairing of a purine-rich sequence of the mRNA with the 3′-terminal tail of 16S ribosomal RNA (rRNA) in the 30S subunit—the Shine-Dalgarno interaction (Shine and Dalgarno, 1974). Interactions between 16S rRNA and mRNA also appear to play a fundamental role in the accuracy of tRNA selection, in which nucleotides G530, A1492, and A1493 have recently been shown to make intimate contact with the codon-anticodon helix in the 30S subunit A site (Ogle et al., 2001). The ribosome is also directly involved in coupled translocation of the mRNA and tRNAs (Belitsina et al., 1981; Gavrilova et al., 1976; Pestka, 1967). Little is known of the molecular mechanisms underlying this process, which must somehow avoid slippage of the translational reading frame during movement. Finally, scant attention has been paid to the mechanism by which the ribosome unwinds secondary structure in the mRNA. The failure of this process may underlie the observed stimulation of translational frame shifting by certain mRNA pseudoknot structures located downstream from the A-site codon (Alam et al., 1999; Brierley et al., 1989), again by an unknown mechanism. Knowledge of the molecular interactions between mRNA and the ribosome will be essential for understanding the mechanistic basis for all of these processes. Apart from certain specific regulatory interactions, most ribosomal contacts must, of necessity, be insensitive to mRNA sequence, and so are expected to involve the mRNA backbone, rather than its bases.

Early nuclease protection studies provided the first indications of the size of the mRNA binding site on the ribosome. Ribonuclease A digestion of R17 phage mRNA bound to the ribosome at the initiation sites of its three cistrons yielded protected fragments about 31 nucleotides in length (Steitz, 1969). A larger region was found to be protected from hydroxyl radicals in chemical footprinting studies using phage T4 gene 32 mRNA, in which the protected region extended some 10–20 nucleotides further at the 3′ end (Hüttenhofer and Noller, 1994). Shatsky et al. (1991) proposed a specific model for the path of the mRNA, based mainly on immuno-EM data in which the mRNA wraps around the neck of the 30S subunit, with its 5′ end on the platform side and its 3′ end near the shoulder. The basic features of the Shatsky-Bogdanov model were retained in the proposal for an mRNA channel (Frank et al., 1995) based on ribosome morphology and the positions of tRNAs in the ribosome as observed in cryoelectron microscopic reconstructions. Brimacombe, Bogdanov, Wollenzein, and their collaborators used directed crosslinking methods to locate individual nucleotides of the ribosome-bound mRNA in relation to specific features of 16S rRNA and ribosomal proteins (Bhangu et al., 1994; Bhangu and Wollenzien, 1992; Brimacombe, 1995; Dokudovskaya et al., 1993; Dontsova et al., 1992; Greuer et al., 1999; Juzumiene et al., 1995; Rinke-Appel et al., 1993, 1994; Sergiev et al., 1997). Within the limits of the knowledge of ribosome structure, these different approaches were in agreement with the original proposal (Shatsky et al., 1991).

In this study, we directly map the path of the mRNA in the ribosome by X-ray crystallography. Using diffraction data from crystals of 70S ribosomal complexes containing bound tRNAs and either a model mRNA fragment or no mRNA at all (Belitsina et al., 1981), we calculate Fourier difference maps of the bound mRNA. Together with the recently reported positions of the A- and P-site codons bound to their respective tRNAs in 70S complexes (Yusupov et al., 2001), we are able to describe the complete path of the mRNA through the ribosome, at 7 Å resolution. The mRNA is threaded through a channel that wraps around the neck of the 30S subunit, confirming the general features of the previous models (Frank et al., 1995; Shatsky et al., 1991). The locations in the ribosome of the Shine-Dalgarno and downstream regions of the mRNA flanking the A and P sites have implications for translational initiation, frame shifting, and other functional interactions of mRNA. Unexpect-

[3] Correspondence: harry@nuvolari.ucsc.edu
[4] Present Address: UPR 9004 de Biologie et de Genomiques Structurales du CNRS, IGBMC B.P. 163, 1 rue L. Fries, 67404 Illkirch Cedex - CU de Strasbourg, France.

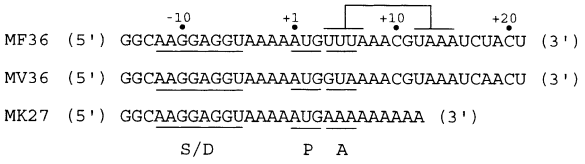

Figure 1. Nucleotide Sequences of the Three Model mRNAs Used in this Study

The Shine-Dalgarno sequence (S/D), and P- and A-site codons are underlined. The self-complementary sequences forming the putative A-site helix in MF36 mRNA are overlined.

edly, a model mRNA based on gene 32 mRNA forms an electron-dense mass, most likely resulting from formation of a small hairpin loop by intramolecular base pairing of the mRNA, that appears to mimic binding of the anticodon loop of tRNA to the A site. Finally, the arrangement of ribosomes around the crystallographic 4-fold axis permits direct threading of the mRNA from one ribosome to the next, suggesting how ribosomes may pack in polysomes to make efficient use of shared mRNA and tRNAs.

Results

The model mRNA MF36 was based on phage T4 gene 32 mRNA (Figure 1), except that the potential for pairing of its Shine-Dalgarno sequence was increased to eight base pairs by extending its complementarity to the 3′ tail of 16S rRNA. For the MV36 and MK27 mRNAs, different coding and downstream regions were also introduced (Figure 1). Complexes containing *Thermus thermophilus* 70S ribosomes, mRNA fragments, and either full-length tRNA or an anticodon stem-loop (ASL) bound to the ribosomal P site were cocrystallized as described (Cate et al., 1999; Yusupov et al., 2001). Similar cocrystals containing 70S ribosomes and initiator tRNA, but lacking mRNA (Belitsina et al., 1981) were prepared under the same conditions. Data were collected using synchrotron radiation, and previously derived structure factor phases (Cate et al., 1999; Yusupov et al., 2001) were used to compute Fourier difference maps (Table 1).

Figure 2A shows the 7 Å Fourier difference map computed for the MK27 mRNA fragment using data collected from crystals containing two types of ribosomal constructs. In one construct, 70S ribosomes were bound with the MK27 mRNA and initiator tRNA; the other construct was identical, except that mRNA was omitted. Pseudoatom models for the mRNA 27-mer and the 3′ terminus of 16S rRNA, as well as the previously determined models for the A and P codons (Yusupov et al., 2001), are shown superimposed on the difference map. The positions of the A and P codons provide a close check on the register of the central part of the mRNA model, while the resolution of the difference map itself allows fitting the rest of the mRNA with a precision of about +/− 1 nucleotide. A pronounced cylinder of electron density is seen at the 5′ end of the mRNA, whose dimensions are in good agreement with the predicted eight base-pair Shine-Dalgarno helix. A gap of about four nucleotides in the electron density is seen at the position of the P codon and its 5′ flanking nucleotide (mRNA positions −1 to +3). This can be explained by the folding back of the 3′ tail of 16S rRNA in the absence of mRNA, as found in the high-resolution structure for the *T. thermophilus* 30S subunit (Wimberly et al., 2000); binding of the tail of 16S rRNA to the P codon position of the ribosome results in subtraction of the P codon from the mRNA difference map. An additional small gap is found at position −4 of the mRNA, which may be due to local disorder. The location of the A codon is close to that found in the presence of A-tRNA, even though A-tRNA was absent in these complexes. At its 3′ end, the MK27 difference density terminates in good agreement with the predicted position of the 3′ end (position +12) of the mRNA model.

The difference map for the MF36 mRNA resembles that of the MK27 mRNA, except at its 3′ tail and in the A codon region, where a cylinder of density overlapping with the position normally occupied by the A-tRNA (Cate et al., 1999; Ogle et al., 2001; Yusupov et al., 2001) appears (Figure 2B). This unexpected feature can be explained by intramolecular base pairing of complementary sequences in the gene 32 mRNA (positions +4 to +7 and +12 to +15 of the MF36 mRNA; Figure 1). This feature is absent in the difference map for MK27 (Figure 2A), in which the self-complementary sequences were replaced by poly(A). A four base-pair stem modeled from a tetraloop-containing helix can be accommodated in the extra difference density (Figure 2B). Modeled in this way, the 3′ end of the MF36 mRNA terminates close to the end of the strongest part of the electron density (Figure 2B). Weaker density can be seen extending about six nucleotides further, suggesting that the unfolded form of the MF36 mRNA is also present, but at lower occupancy. The weaker density extends to about position +17, implying that the very 3′ end of the mRNA

Table 1. Crystallographic Data[a]

Data set (model mRNA)	no mRNA	MK27	MF36	MV36
High-resolution limit (Å)	6.5	5.6	5.0	7.0
R_{sym}*	8.9	12.4	9.4	8.8
Mean I/σ(I)	2.6 at 6.5 Å	2.1 at 5.6	3.3 at 5.5	2.3 at 7.0
Number of reflections				
Unique	95,127	153,627	209,044	73,146
Observational redundancy	3.6	3.0	2.8	3.6
Completeness (%)	96.7	97.7	95.3	89.5

[a] Crystals of ribosomal complexes were prepared as described in Experimental Procedures, using the model mRNAs MK27, MF36, and MV36 (Figure 1). All data were collected at beamline 5.0.2, at the Berkeley Center for Structural Biology, Lawrence Berkeley National Laboratory.
*$R_{sym} = \Sigma \mid I - \langle I \rangle \mid / \Sigma I$

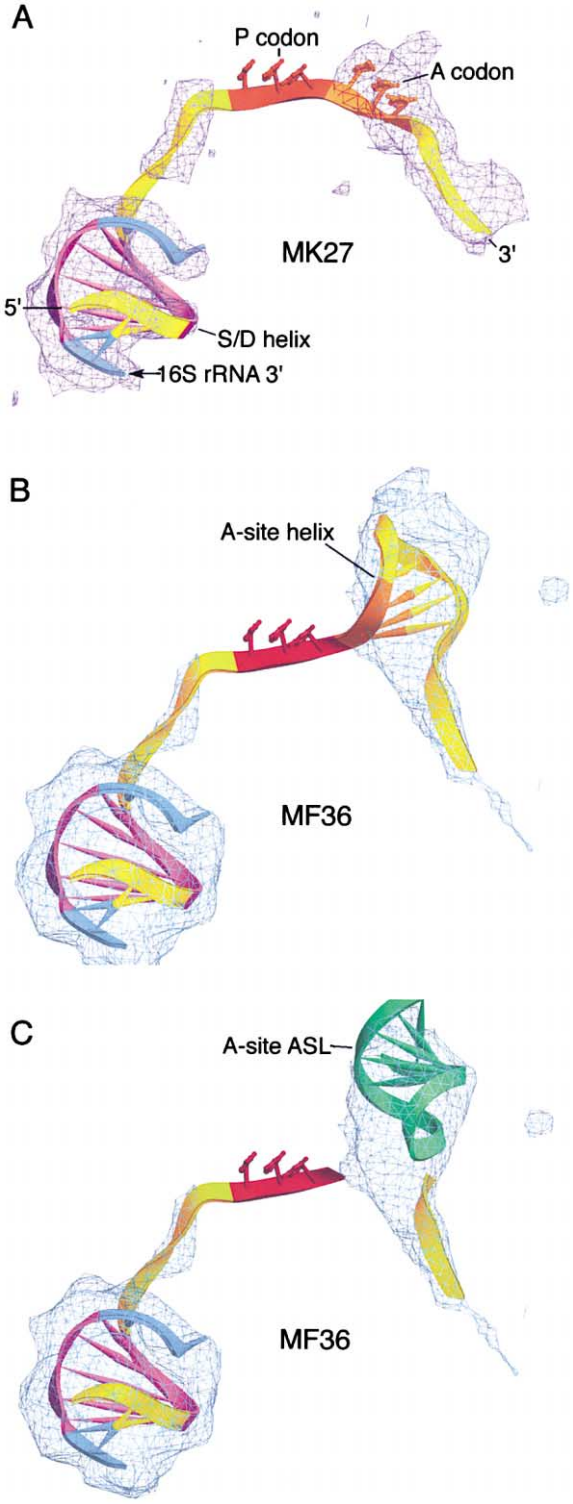

Figure 2. Fourier Difference Maps of mRNAs

(A) 7 Å Fourier difference map of MK27 mRNA with the mRNA model (yellow) docked, showing the position of the Shine-Dalgarno (S/D) helix (magenta) and the positions of the A- and P-site codons (orange and red, respectively), viewed from the top of the 30S ribosomal subunit.

(B) Difference map of the MF36 mRNA, showing a four-base-pair tetraloop helix (A-site helix) fitted to the extra density at the A site.

(C) Same as for (B), except that the A-tRNA anticodon stem-loop (green) is shown in the position observed experimentally in the A-tRNA difference map (Yusupov et al., 2001), in place of the A-site mRNA helix. The five-nucleotide (GGAGG/CCUCC) core of the Shine-Dalgarno interaction is shown in magenta, and the rest of the 16S rRNA tail in cyan.

chain (nucleotides +18 through +21) is disordered in the unfolded mRNA conformer. The mRNA hairpin feature occupies the position of the anticodon stem-loop (ASL) of the A-site tRNA (Cate et al., 1999; Yusupov et al., 2001), as shown in Figure 2C. The striking coincidence of these two structures suggests that the mRNA hairpin may be designed to mimic the A-site ASL, possibly playing a role in initiation of translation of gene 32 mRNA.

Figure 3A shows the path of the mRNA in the context of the complete 30S ribosomal subunit of the 70S ribosome, as viewed from the subunit interface. The mRNA passes through upstream and downstream tunnels to access the interface, where only about eight nucleotides (−1 to +7), centered on the junction between the A and P codons, are exposed. Binding of mRNA to the 30S subunit during translational initiation requires opening one or both of the tunnels (which are closed noncovalently) depending on the length of the upstream leader, since it has been shown by Bretscher (1968) that the ribosome is able to initiate translation on a circular message. The contact point between the head and body has been described as a potential "latch," the closing of which was proposed to provide a geometry that guarantees processivity, provides directionality, and prevents dissociation (Schluenzen et al., 2000). The boundaries of the ribosomal contacts with the mRNA (−15 to +16) are within experimental error of those predicted (−16 to +16) by Steitz (1969). The features of 16S rRNA structure that surround the message agree well (P-P distances from 8 to 28 Å) with all but one (60Å between mRNA position −1 to −8 with 16S rRNA position 1360) of the site-directed crosslinking results in which both the mRNA and rRNA crosslinking positions were characterized (Bhangu et al., 1994; Brimacombe, 1995; Dokudovskaya et al., 1993; Dontsova et al., 1992; Greuer et al., 1999; Juzumiene et al., 1995; Rinke-Appel et al., 1993, 1994; Sergiev et al., 1997). The 5′ end of the mRNA originates at the back of the platform (Figure 3B), where it enters the groove between the head and platform, wrapping around the neck of the subunit and exiting on the opposite side between the head and shoulder. Although the ribosome-bound portion of the mRNA contains about 30 nucleotides, stretching from about position −15 to +15, the region most closely wrapped around the neck extends from around positions −3 to +10, centering on the junction between the A and P codons. The immediate molecular environment of the mRNA contains mainly 16S rRNA (Figure 3A), except at the extremities of its binding site, around the upstream Shine-Dalgarno interaction and in the downstream region around position +12, as well as in the A codon, where it is close to ribosomal proteins.

Upstream Interactions

The Shine-Dalgarno helix fits into a large cleft between the back of the platform and the head of the subunit

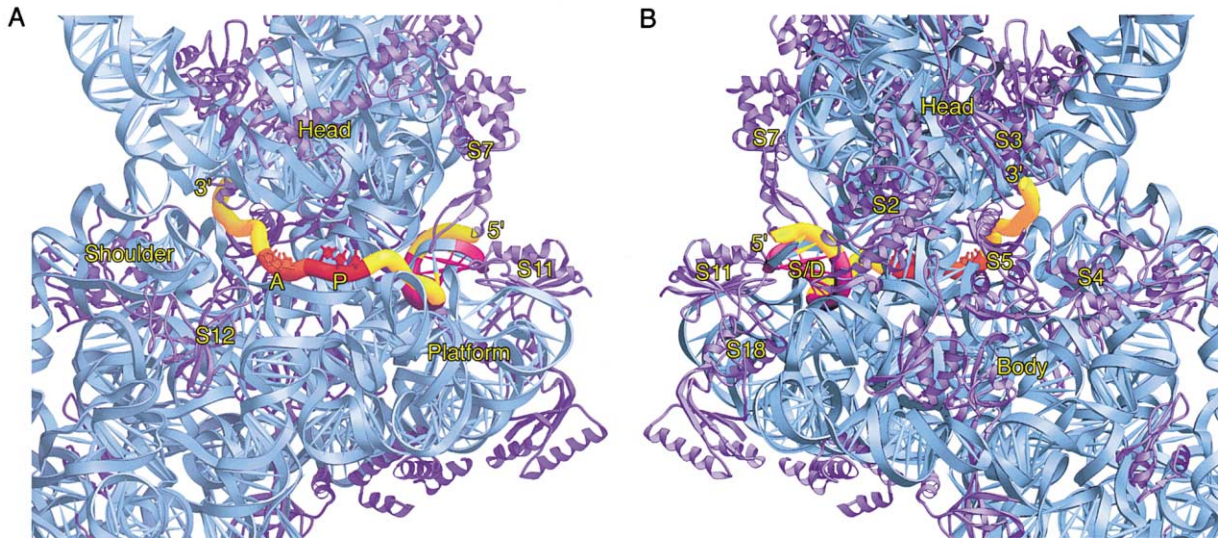

Figure 3. Path of mRNA through the 30S Ribosomal Subunit

(A) Interface and (B) solvent views of the mRNA in the 30S ribosomal subunit. A, P; the A- and P-site codons. 5′, 3′; the 5′ and 3′ correspond to positions −15 and +15 of the mRNA model. The head, platform, shoulder, and body of the subunit, and ribosomal proteins S2, S3, S4, S5, S7, S11, S12, and S18 are indicated. The ribosomal proteins are shown in dark blue, 16S rRNA in cyan and the mRNA is colored as in Figure 2.

(Figure 4A). In the solvent-side view, The Shine-Dalgarno cleft is formed by helix 20 on the bottom, the 723 bulge loop and proteins S11 and S18 on the left, and the neck helix (helix 28) and helix 37 on the right. The N-terminal end of protein S18, which is rich in basic and aromatic side chains, is directed toward the major groove of the Shine-Dalgarno helix, at the 5′ end of the mRNA (position –15). Extra density under the upstream end of the Shine-Dalgarno helix may come from the N-terminal 15 amino acids of S18, which were disordered in the high-resolution structure of the 30S subunit (Wimberly et al., 2000). Both the N-terminal tail and the loop of S11 that contains Arg 54 are near enough to make specific interactions with the Shine-Dalgarno helix. At the downstream end of the Shine-Dalgarno helix, the C-terminal tail of protein S11 interacts with the backbone of the mRNA around positions −4 to −6.

Directly downstream of the Shine-Dalgarno helix, the 5′ leader (positions −1 to −4) of the mRNA passes through a short tunnel between the head and the platform of the subunit to the interface side, where it is surrounded by the tip of the β hairpin of protein S7, the apex of the 690 loop, the minor groove side of the 790 loop, the base of helix 45 around position 1505, and the 925 region of helix 28. This region of the mRNA contains the E codon (position −1 to −3), whose full access to the interface is hindered by its location in the tunnel.

The P and A Codons

After a sharp turn in the mRNA around position −1, the P and A codons are presented to their respective tRNAs in the middle of the interface surface of the cleft, with an approximately 45° kink between the adjacent codons that allows simultaneous pairing of the A- and P-tRNA anticodons (Yusupov et al., 2001). The two codons are centered above the axis of the penultimate stem of 16S rRNA, where they occupy the major groove of the noncanonical helical structure formed by the 1400 and 1500 strands of 16S rRNA often referred to as the "decoding site" (Figure 4B). As noted above, the P codon follows a path very similar to that described for the folded-back tail of 16S rRNA, which appears to mimic this region of the mRNA in the high-resolution crystal structure of the 30S subunit (Wimberly et al., 2000).

Some details of the interactions between the ribosome and the P codon can therefore be inferred from the 30S structure. Interestingly, the N1 position of G926, which was protected from kethoxal by P-tRNA binding, even in the absence of mRNA (Moazed and Noller, 1986, 1990), is positioned to interact with the phosphate of nucleotide +1 of the P codon. The observed tRNA-dependent protection may be due to repositioning of the mRNA chain (or the 16S tail, in the absence of mRNA) in response to tRNA binding, since the mRNA backbone begins to diverge from the path of the 3′ tail of 16S rRNA near position −1 of the mRNA. Modification interference experiments also indicated the importance for G926 in mRNA-independent binding of $tRNA^{Phe}$ to the 30S P site (von Ahsen and Noller, 1995); since the 3′ tail does not contain a Phe codon, this result suggests that the apparent mRNA mimicry by the 16S rRNA tail, stabilized by the 926 interaction, may be important in inducing the active conformation of the 30S P site, and could help to explain the fact that initiator tRNA can bind to the 30S subunit independently of mRNA during translational initiation (Gualerzi et al., 1977).

The 1500 strand of 16S rRNA crosses at right angles to the mRNA chain, where nucleotide 1498 lies directly under nucleotide +1 of the P codon (Figure 4B). In the high-resolution structure (Wimberly et al., 2000) the phosphate of nucleotide 1498 packs against ribose +1 and its base (m^3U 1498 in *E. coli*) against ribose +2.

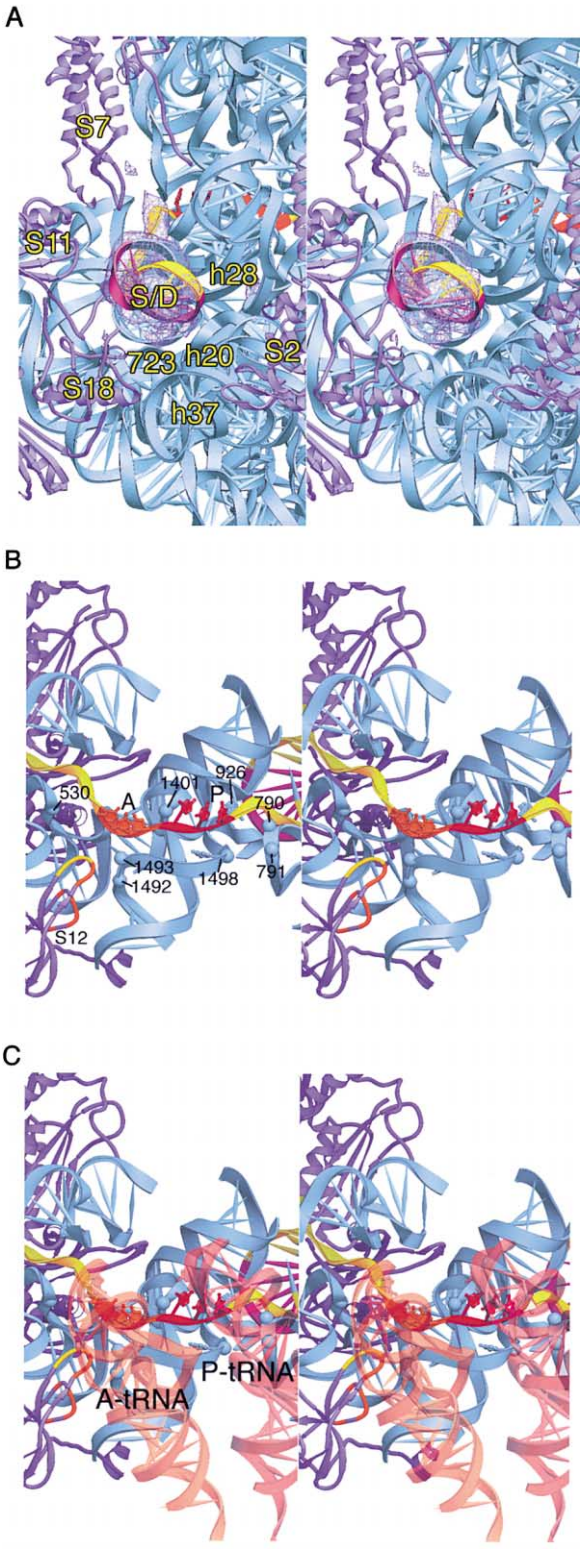

Figure 4. Detailed Views of mRNA-Ribosome Interactions

(A) Solvent-side stereo view of the Shine-Dalgarno (S/D) helix bound in its cleft, formed by helices 20, 28, and 37 (h20, h28, h37) and the 723 loop of 16S rRNA and proteins S11 and S18, and the path of mRNA nucleotides −1 to −4 through the upstream tunnel. The MV36 Fourier difference map is shown.

(B) Interface stereo view of the A- and P-site codons and their flanking nucleotides (530, 790, 791, 926, 1492, 1493, and 1498) in 16S rRNA. The locations of restrictive mutations in ribosomal protein S12 are shown in yellow (the universal PNSA sequence) and orange. The positions of the bases for G926 and U1498 are modeled from the high-resolution structure of the *T. thermophilus* 30S subunit (Wimberly et al., 2000).

(C) Same as (B), but with the A- and P-tRNAs (orange and red, respectively) docked according to their experimentally observed locations (Yusupov et al., 2001).

These interactions are evidently stabilized by interaction of the N6-amino group of A790 and the N1 of the universally conserved G791 with the nonbridging phosphate oxygens of nucleotide 1498. Both A790 and G791 were earlier identified as "class III" bases (Moazed and Noller, 1987), whose protection from attack by chemical probes at their N1 positions was predicted to result from a conformational change in 16S rRNA, because the same protections were conferred by P-tRNA, 50S subunits, or certain antibiotics. These class III protections can now be explained by movement of the 790 stem-loop (helix 24) toward the penultimate stem in response to binding of P-tRNA or the other ligands, simultaneously resulting in interaction of the backbone of the 790 loop with the bottom of the anticodon stem of P-tRNA and packing of nucleotide 1498 against the P codon. Such a movement would be consistent with the counterclockwise rotation of the platform of the 30S subunit when it joins with the 50S subunit, observed in cryo-EM studies (Lata et al., 1996).

At the junction between the P and A codons, the mRNA is blocked from continuing its A-RNA-like trajectory by the phosphate of nucleotide 1401, which lies directly in its path (Figure 4B). This redirects the mRNA, resulting in the observed kink in the mRNA between the A and P codons.

In the A site, the bases G530, A1492, and A1493 interact intimately with the minor groove of the A-site codon-anticodon helix, in a possible discriminatory mechanism for A-site tRNA selection, as shown recently by Ramakrishnan and coworkers (Ogle et al., 2001). A further interaction is made by the β-hairpin loop of protein S12 around the conserved PNSA sequence at positions 48–51, which is directly beneath riboses +5 and +6 (Ogle et al., 2001). This part of S12 contains most of the mutations that confer restrictive (hyperaccurate) phenotypes.

Downstream Interactions

Immediately downstream of the A codon, the mRNA passes through a second tunnel, about 20 Å in diameter, between the head and shoulder of the subunit, leading to the solvent side of the 30S subunit, first observed in cryo-EM reconstructions (Frank et al., 1995). It has been suggested that closing of this tunnel around the mRNA ensures processivity and directionality of mRNA movement (Schluenzen et al., 2000). From the interface side, the mRNA (positions ca. +7 to +10) passes first through a layer of RNA, where it is surrounded by helix 34 at the top, the base of the neck at nucleotide 1397 (helix 28) on the right, the 5′ hairpin loop (at nucleotide 16 of 16S rRNA) at the bottom, and the 530 loop on the left (Figure 5A). In the RNA layer, bases C1397 and U1196 (Wimberly

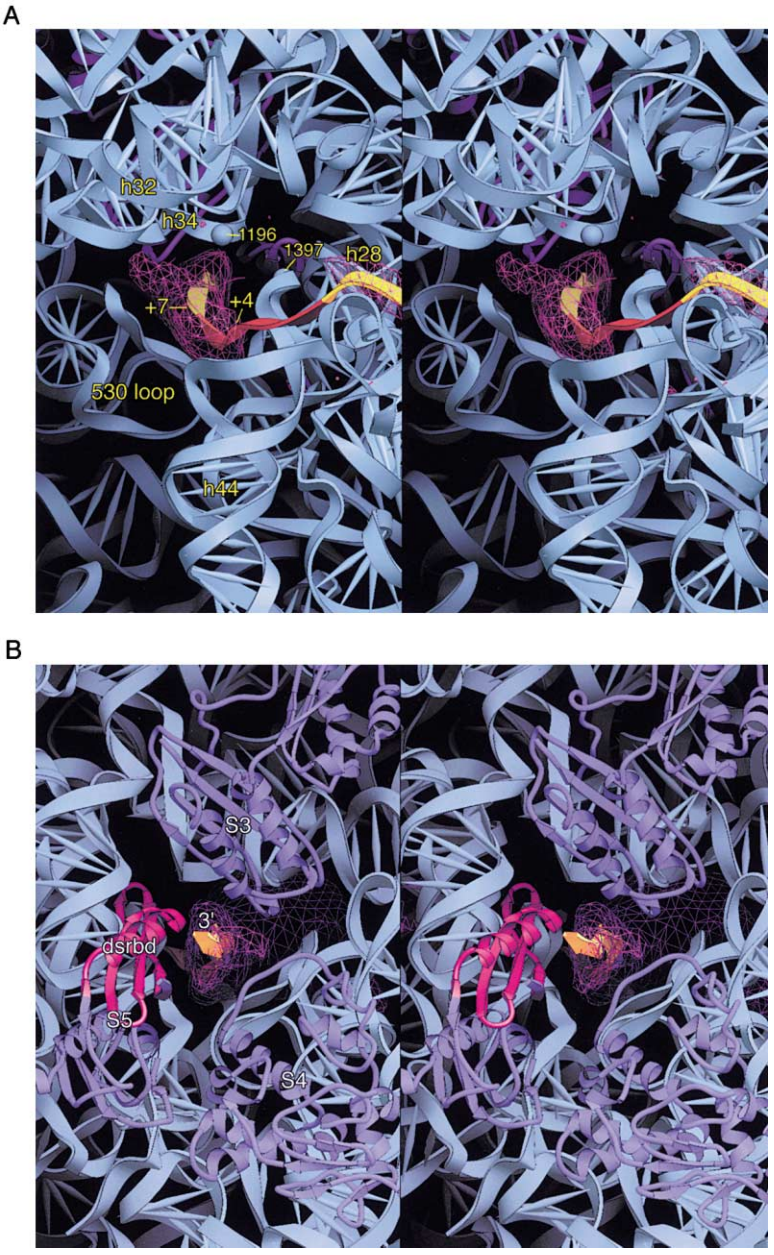

Figure 5. The Downstream Tunnel

(A) Interface stereo view of the downstream tunnel, showing the features of 16S rRNA layer surrounding mRNA positions +7 to +10. (B) Solvent-side stereo view of the downstream tunnel, showing the formation of the protein layer surrounding positions +11 to +15 of the mRNA by proteins S3, S4, and S5. The double-stranded RNA binding domain of protein S5 is shown in magenta. The MK27 difference map is shown.

et al., 2000) are oriented toward the mRNA around positions +7 and +9, respectively, and may help to position the mRNA immediately downstream from the A codon.

Finally, the mRNA (positions approximately +11 to +15) passes through a layer of protein into the solvent at the back of the subunit. Viewed from the solvent side (Figure 5B), the mRNA is encircled by protein S3 at the top, S4 on the right, and S5 on the lower left. These three proteins project a dense array of basic side chains into the downstream tunnel, including Arg131, Arg132, Lys135, and Arg164 from S3; Arg47, Arg49, and Arg50 from S4; and Arg15 and Arg24 from S5, which appear to position the downstream region of the mRNA via interactions with its backbone phosphates.

mRNA Helices, Pseudoknots, and Frame Shifting

All mRNA chains have the ability to form hairpins and other intramolecularly base-paired structures, yet the codons must be read in single-stranded form. The ribosome is therefore able to unwind mRNA secondary structure by some as-yet unknown mechanism. An mRNA hairpin would approach the ribosome surface at the back of the 30S subunit, from the view shown in Figure 5B. Since an RNA helix is too large to pass through the narrow downstream tunnel, unwinding of mRNA structure is likely to occur at or near the entrance to the tunnel, around positions +13 to +15. (Unfolding of a downstream [+11 to +17, +25 to +31] hairpin of λ cro mRNA, dependent on binding of initiator tRNA, may result from its threading through the downstream tunnel [Balakin et al., 1990].)

A possible mechanistic basis for an mRNA helicase is suggested by the fact that proteins S4 and S5 are integral to the body of the 30S subunit, whereas S3 is part of the head. If one strand of the incoming helix were bound to S4 and/or S5 and the other strand to S3, the

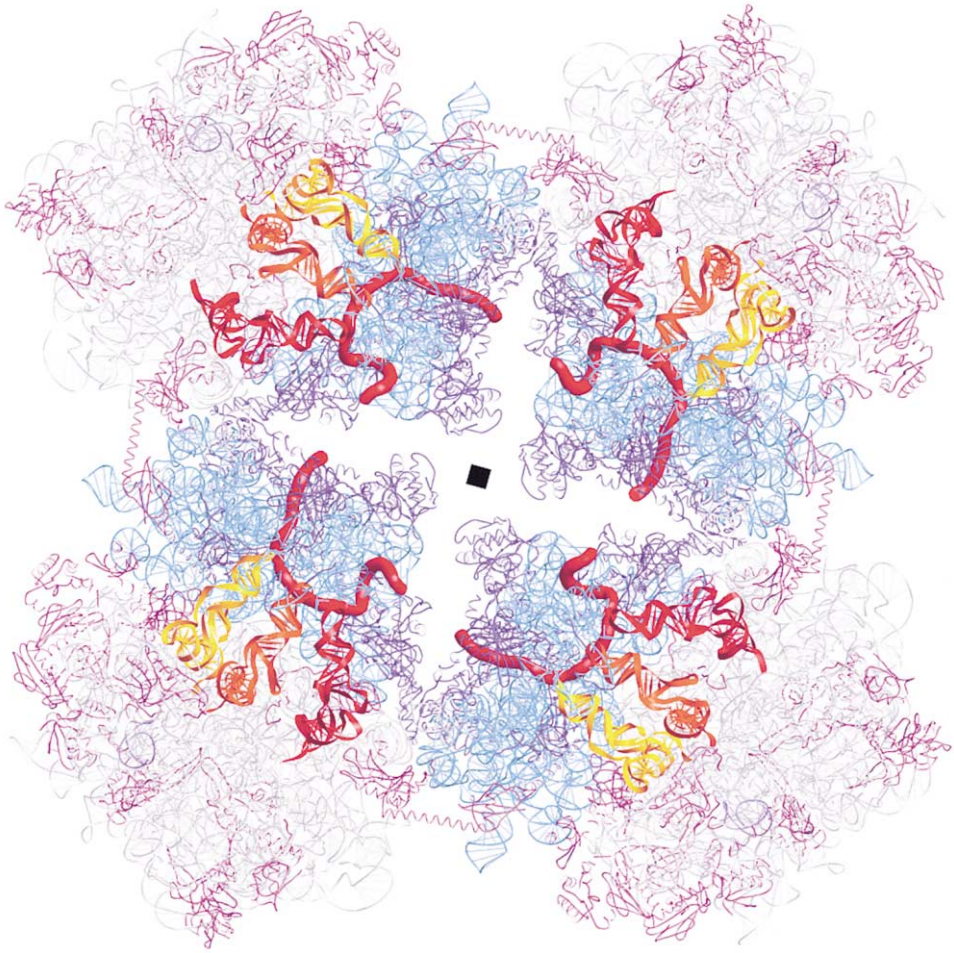

Figure 6. Arrangement of Ribosomes and mRNA in the Crystal

View down the crystallographic 4-fold axis of the 70S ribosome-mRNA-tRNA complex (Yusupov et al., 2001), showing the head-to-tail juxtaposition of the model mRNAs (red-orange) between adjacent ribosomes. The molecular components shown are 16S rRNA (cyan), 23S rRNA (gray), 5S rRNA (gray-blue), small subunit proteins (dark blue), large subunit proteins (magenta), the A-, P-, and E-tRNAs (yellow, orange, and red), and the mRNA (red-orange).

rotational movement of the head that is believed to occur during translocation (Agrawal et al., 1999) could result in physical disruption of the helix, at the rate of about three base pairs (i.e., one codon) at a time, simultaneously advancing the mRNA through the ribosome. Interestingly, the part of protein S5 that faces the mRNA near its entry point to the downstream tunnel has the same three-dimensional fold as the double-stranded RNA binding domain (dsRBD) (Ryter and Schultz, 1998). However, its relatively low sequence homology with the dsRBD consensus does not provide support for its potential binding to double-stranded RNA (dsRNA), at least in the way that has been observed for complexes containing the *Xenopus* Xlrbpa protein and dsRNA (Ryter and Schultz, 1998).

One type of structure that has been shown to perturb translation are mRNA pseudoknots. Most extensively documented is the finding that certain downstream pseudoknots promote a −1 shift of the translational reading frame when a "shifty" sequence is positioned in the decoding site, a mechanism that is exploited for translational regulation by many viruses (Alam et al., 1999; Brierley et al., 1989). The optimum position for the pseudoknot is between positions +11 and +15, which corresponds closely to the region where mRNA enters the downstream tunnel (+13 to +15), at the position of the proposed mRNA helicase. A simple explanation for the frameshifting event is that the structure of the pseudoknot is poorly matched to the geometry of the helicase, blocking entry of the mRNA into the downstream tunnel. Upon EF-G-catalyzed translocation, forward movement of the mRNA would be retarded, resulting in backlash of the mRNA and favoring slippage into the −1 reading frame.

Path of the mRNA in the Crystal Lattice

In our crystals, the *Thermus thermophilus* 70S ribosomes pack in the I422 tetragonal space group (Cate et al., 1999), in which adjacent ribosomes are organized symmetrically in layers of tetramers that are centered around a 4-fold axis. Figure 6 shows the arrangement of ribosomes around the 4-fold axis in the crystal lattice. A striking feature of this arrangement is that it juxtaposes the 3′ end of the mRNA in one 70S monomer with the

5′ end of the mRNA of the adjacent 70S monomer, in principle permitting direct threading of a single continuous mRNA through all four ribosomes in the tetramer. The crystal packing might reflect one of the ways in which ribosomes interact with each other in polysomes in vivo. An interesting consequence is that this places the E site of one ribosome directly adjacent to the A site of its neighboring ribosome. The result would be to increase the local concentration of cognate tRNA in the vicinity of the A site of the adjacent ribosome. Moreover, this would hold for many different orientations of adjacent ribosomes bound to the same mRNA. The implications of this observation are not yet clear; for example, it is necessary to aminoacylate the discharged tRNA before it can be bound by the next ribosome, requiring the presence of its cognate synthetase. Nevertheless, simplifying the task of sorting through the more than 50 different tRNA species, even incrementally, could help reduce the considerable energetic costs of maintaining translational accuracy.

Conclusion

Although most of the atomic details of mRNA-ribosome interaction are yet to be resolved, our 7 Å difference maps clearly reveal the path of the mRNA through the ribosome and allow identification of the molecular features of the ribosome that surround each position along the length of the mRNA. The path taken by mRNA through the *T. thermophilus* 70S ribosome is likely to be generalizable to all bacterial and archaeal ribosomes, which share all of the structural features making up the mRNA binding channel. In fact, with the exception of the Shine-Dalgarno interaction, which is absent in eukaryotic ribosomes, we would expect mRNAs to follow a very similar path in all ribosomes. A major unanswered question is how the movement of mRNA is coupled to tRNA movement during the translocation step of protein synthesis, to prevent disruption of the weak codon-anticodon interactions and loss of the translational reading frame. A possible answer is that some of the ribosomal features that contact the mRNA are themselves mobile, and that the ribosome is able to coordinate their movement with that of tRNA during translocation. A possible example, mentioned above, is the head of the 30S subunit. Another obvious candidate is the decoding site itself, a noncanonical helix that links the penultimate stem with the head of the small subunit. The A and P codons are threaded through the major groove of this unusual helix (Figure 4B), which is formed from the universally conserved 1400 and 1500 strands of 16S rRNA. The decoding site helix is, in turn, connected via bridge B2a to another noncanonical helix formed by the universally conserved 1935 and 1965 strands of 23S rRNA in the lateral arm of domain IV, that has been proposed to play a role in tRNA movement and intersubunit signaling (Yusupov et al., 2001). Intriguingly, the connection between the two noncanonical helices is made by helix 69 of 23S rRNA, which not only interacts via its hairpin loop to the decoding site of 16S rRNA, but simultaneously interacts with the D stems of both the A- and P-tRNAs, suggesting a possible structural basis for coupling mRNA and tRNA translocation. The structural studies presented here and elsewhere should help to provide a basis for designing strategies to test emerging models for the molecular basis of ribosomal dynamics.

Experimental Procedures

Model mRNA Constructs

Model mRNAs were based initially on the phage T4 gene 32 mRNA. For all three mRNAs (Figure 1), the Shine-Dalgarno pairing was increased to allow eight potential base pairs with 16S rRNA, and a GGC sequence originally added to the 5′ end to facilitate transcription by T7 RNA polymerase. The mRNA samples used in these studies were made by solid-phase synthesis (Dharmacon, Inc., Boulder, CO), and gel purified prior to use in crystallization.

Crystallization, Data Collection, and Model Fitting

Thermus thermophilus 70S ribosomes were prepared and cocrystallized with purified *E. coli* initiator tRNA (Subriden, Rollingbay, WA) and MK27, MF36, or MV36 mRNAs (Dharmacon), or without mRNA, using the same conditions reported previously (Cate et al., 1999; Yusupov et al., 2001). Diffraction data were collected using synchrotron radiation, as previously described (Cate et al., 1999), and processed using Scalepack and Denzo (Otwinowski, 1993). Fourier difference maps were calculated from measured native amplitudes (Table 1) and previously calculated structure factor phases (Cate et al., 1999; Yusupov et al., 2001) using the CCP4 suite of programs (1994). mRNA models were fitted using O (Jones and Kjeldgaard, 1997), and molecular structure figures were rendered using Ribbons (Carson, 1997).

Acknowledgments

We thank Albion Baucom for preparing the molecular graphics figures and Thomas Earnest for continuing help and advice at beamline 5.0.2 at the Berkeley Center for Structural Biology, LBNL. This work was supported by grants from the NIH and the Agouron Institute (to H.F.N) and from the W.M. Keck Foundation (to the Center for Molecular Biology of RNA). The Macromolecular Crystallography Facility at the Advanced Light Source, Lawrence Berkeley National Laboratory is supported by the Department of Energy and by grants from the NIH and the Agouron Institute.

Received May 15, 2001; revised June 25, 2001.

References

Agrawal, R.K., Heagle, A.B., Penczek, P., Grassucci, R.A., and Frank, J. (1999). EF-G-dependent GTP hydrolysis induces translocation accompanied by large conformational changes in the 70S ribosome. Nat. Struct. Biol. *6*, 643–647.

Alam, S.L., Atkins, J.F., and Gesteland, R.F. (1999). Programmed ribosomal frameshifting: much ado about knotting! Proc. Natl. Acad. Sci. USA *96*, 14177–14179.

Balakin, A., Skripkin, E., Shatsky, I., and Bogdanov, A. (1990). Transition of the mRNA sequence downstream from the initiation codon into a single-stranded conformation is strongly promoted by binding of the initiator tRNA. Biochim. Biophys. Acta *1050*, 119–123.

Belitsina, N.V., Tnalina, G.Z., and Spirin, A.S. (1981). Template-free ribosomal synthesis of polylysine from lysyl-tRNA. FEBS Lett. *131*, 289–292.

Bhangu, R., and Wollenzien, P. (1992). The mRNA binding track in the Escherichia coli ribosome for mRNAs of different sequences. Biochemistry *31*, 5937–5944.

Bhangu, R., Juzumiene, D., and Wollenzien, P. (1994). Arrangement of messenger RNA on Escherichia coli ribosomes with respect to 10 16S rRNA cross-linking sites. Biochemistry *33*, 3063–3070.

Bretscher, M.S. (1968). Direct translation of a circular messenger DNA. Nature *220*, 1088–1091.

Brierley, I., Digard, P., and Inglis, S.C. (1989). Characterization of an efficient coronavirus ribosomal frameshifting signal: requirement for an RNA pseudoknot. Cell *57*, 537–547.

Brimacombe, R. (1995). The structure of ribosomal RNA: a three-dimensional jigsaw puzzle. Eur. J. Biochem. *230*, 365–383.

Carson, M. (1997). Ribbons. Methods Enzymol. *277B*, 493–505.

Cate, J.H., Yusupov, M.M., Yusupova, G.Z., Earnest, T.N., and Noller, H.F. (1999). X-ray crystal structures of 70S ribosome functional complexes. Science *285*, 2095–2104.

Collaborative Computing Project Number 4. (1994). Acta Crystallogr. *D50*, 760–763.

Dokudovskaya, S.S., Dontsova, O.A., Bogdanova, S.L., Bogdanov, A.A., and Brimacombe, R. (1993). mRNA-ribosome interactions. Biotechnol. Appl. Biochem. *18*, 149–155.

Dontsova, O., Dokudovskaya, S., Kopylov, A., Bogdanov, A., Rinke-Appel, J., Junke, N., and Brimacombe, R. (1992). Three widely separated positions in the 16S RNA lie in or close to the ribosomal decoding region; a site-directed cross-linking study with mRNA analogues. EMBO J. *11*, 3105–3116.

Frank, J., Zhu, J., Penczek, P., Li, Y., Srivastava, S., Verschoor, A., Radermacher, M., Grassucci, R., Lata, K.R., and Agrawal, R.K. (1995). A model of protein synthesis based on cryo-electron microscopy of the *E. coli* ribosome. Nature *376*, 441–444.

Gavrilova, L.P., Kostiashkina, O.E., Koteliansky, V.E., Rutkevitch, N.M., and Spirin, A.S. (1976). Factor-free ("non-enzymic") and factor-dependent systems of translation of polyuridylic acid by Escherichia coli ribosomes. J. Mol. Biol. *101*, 537–552.

Greuer, B., Thiede, B., and Brimacombe, R. (1999). The cross-link from the upstream region of mRNA to ribosomal protein S7 is located in the C-terminal peptide: experimental verification of a prediction from modeling studies. RNA *5*, 1521–1525.

Gualerzi, C., Risuleo, G., and Pon, C.L. (1977). Initial rate kinetic analysis of the mechanism of initiation complex formation and the role of initiation factor IF-3. Biochemistry *16*, 1684–1689.

Hüttenhofer, A., and Noller, H.F. (1994). Footprinting mRNA-ribosome complexes with chemical probes. EMBO J. *13*, 3892–3901.

Jones, T.A., and Kjeldgaard, M. (1997). Electron-density map interpretation. Methods Enzymol. *277B*, 173–208.

Juzumiene, D.I., Shapkina, T.G., and Wollenzien, P. (1995). Distribution of cross-links between mRNA analogues and 16S rRNA in Escherichia coli 70S ribosomes made under equilibrium conditions and their response to tRNA binding. J. Biol. Chem. *270*, 12794–12800.

Lata, K.R., Agrawal, R.K., Penczek, P., Grassucci, R., Zhu, J., and Frank, J. (1996). Three-dimensional reconstruction of the *Escherichia coli* 30S ribosomal subunit in ice. J. Mol. Biol. *262*, 43–52.

Moazed, D., and Noller, H.F. (1986). Transfer RNA shields specific nucleotides in 16S ribosomal RNA from attack by chemical probes. Cell *47*, 985–994.

Moazed, D., and Noller, H.F. (1987). Interaction of antibiotics with functional sites in 16S ribosomal RNA. Nature *327*, 389–394.

Moazed, D., and Noller, H.F. (1990). Binding of tRNA to the ribosomal A and P sites protects two distinct sets of nucleotides in 16S rRNA. J. Mol. Biol. *211*, 135–145.

Ogle, J.M., Brodersen, D.E., Clemons, W.M., Tarry, M.J., Carter, A.P., and Ramakrishnan, V. (2001). Recognition of cognate transfer RNA by the 30S ribosomal subunit. Science *292*, 897–902.

Otwinowski, Z. (1993). In Data Collection and Processing, L. Sawyer, N. Isaacs and D. Bailey, eds. (Warrington, UK: SERC Daresbury Laboratory), pp. 52–62.

Pestka, S. (1967). Studies on the formation of transfer ribonucleic acid-ribosome complexes. II. A possible site on the 50 S subunit protecting aminoacyl transfer ribonucleic acid from deacylation. J. Biol. Chem. *242*, 4939–4947.

Rinke-Appel, J., Junke, N., Brimacombe, R., Dokudovskaya, S., Dontsova, O., and Bogdanov, A. (1993). Site-directed cross-linking of mRNA analogues to 16S ribosomal RNA; a complete scan of cross-links from all positions between '+1' and '+16' on the mRNA, downstream from the decoding site. Nucleic Acids Res. *21*, 2853–2859.

Rinke-Appel, J., Junke, N., Brimacombe, R., Lavrik, I., Dokudovskaya, S., Dontsova, O., and Bogdanov, A. (1994). Contacts between 16S ribosomal RNA and mRNA, within the spacer region separating the AUG initiator codon and the Shine-Dalgarno sequence; a site-directed cross-linking study. Nucleic Acids Res. *22*, 3018–3025.

Ryter, J.M. and Schultz, S.C. (1998). Molecular basis of double-stranded RNA-protein interactions: structure of dsRNA-binding domain complexed with dsRNA. EMBO J. *17*, 7505–7513.

Schluenzen, F., Tocilj, A., Zarivach, R., Harms, J., Gluehmann, M., Janell, D., Bashan, A., Bartels, H., Agmon, I., Franceschi, F., and Yonath, A. (2000). Structure of functionally activated small ribosomal subunit at 3.3 angstroms resolution. Cell *102*, 615–623.

Sergiev, P.V., Lavrik, I.N., Wlasoff, V.A., Dokudovskaya, S.S., Dontsova, O.A., Bogdanov, A.A., and Brimacombe, R. (1997). The path of mRNA through the bacterial ribosome: a site-directed crosslinking study using new photoreactive derivatives of guanosine and uridine. RNA *3*, 464–475.

Shatsky, I.N., Bakin, A.V., Bogdanov, A.A., and Vasiliev, V.D. (1991). How does the mRNA pass through the ribosome? Biochimie *73*, 937–945.

Shine, J., and Dalgarno, L. (1974). The 3′-terminal sequence of E coli 16S ribosomal RNA complementarity to nonsense triplets and ribosome binding sites. Proc. Natl. Acad. Sci. USA *71*, 1342–1346.

Steitz, J.A. (1969). Polypeptide chain initiation: nucleotide sequences of the three ribosomal binding sites in bacteriophage R17 RNA. Nature *224*, 957–964.

von Ahsen, U., and Noller, H.F. (1995). Identification of bases in 16S rRNA essential for tRNA binding at the 30S ribosomal P site. Science *267*, 234–237.

Wimberly, B.T., Brodersen, D.E., Clemons, W.M., Jr., Morgan-Warren, R.J., Carter, A.P., Vonrhein, C., Hartsch, T., and Ramakrishnan, V. (2000). Structure of the 30S ribosomal subunit. Nature *407*, 327–339.

Yusupov, M., Yusupova, G., Baucom, A., Lieberman, K., Earnest, T.N., Cate, J.H., and Noller, H.F. (2001). Crystal structure of the ribosome at 5.5 Å resolution. Science *292*, 883–896.

Accession Numbers

Coordinates for the mRNA structural models have been deposited in the RCSB with PDB accession number 1JGO.